



# A prominent colour front in False Bay, South Africa: Cross-frontal structure, composition and origin

H.N. Waldron<sup>a,\*</sup>, C.K. Wainman<sup>b</sup>, M.E. Waldron<sup>c</sup>, C. Whittle<sup>a</sup>, G.B. Brundrit<sup>a</sup>

<sup>a</sup> Department of Oceanography, University of Cape Town, Rondebosch 7700, South Africa

<sup>b</sup> Institute for Maritime Technology, Martello Rd, Simon's Town, 7995, South Africa

<sup>c</sup> Electron Microscope Unit, University of Cape Town, Rondebosch 7700, South Africa

Received 19 July 2007; accepted 22 October 2007

## Abstract

Colour fronts are a frequent occurrence in False Bay, South Africa, and their occurrence has been the subject of previous study and anecdotal conjecture. The opportunity arose to make a cross-frontal study of this feature in November 2005. Photographs were taken and, subsequently, satellite imagery was obtained. Measurements were made of temperature, salinity, turbidity, dissolved oxygen, suspended solids, plant nutrients and chlorophyll *a*. Cross-frontal comparisons were also made on particulate material using a scanning electron microscope (SEM) and elemental dispersive x-ray (EDX) analysis. Frontal waters were milky white-green in colour, in stark contrast to the adjacent clearer, green-blue waters. The milky white-green water (MW-GW) was found to be warmer, (apparently) less saline, more turbid, richer in nitrate and silicate and had a higher chlorophyll *a* concentration. The dissolved oxygen signal was less pronounced, both water types being supersaturated. Paradoxically, in spite of the higher turbidity in the MW-GW, both water types had similar weights of suspended solids, although the MW-GW material was found to be more abundant and fragmentary when compared with its green-blue water (G-BW) counterpart. The MW-GW was rich in calcium whereas the G-BW was silicon enriched. The central findings of this study are that the strong southerly, onshore wind conditions prior to MW-GW formation introduced calcium-rich, fine particulates into the waters of the surf-zone. The sources of these particulates are thought to be the sea bed sediments and the sea/land interface. The particulates are close to neutral buoyancy enabling the MW-GW to persist over the time-scale of days. A mechanism reinforced by the warming of this water in the nearshore zone. The water was then advected by wind-forcing and subsequently, its own inertia around the north-west corner of False Bay, at which stage it was easily observed and sampled. It is suggested that the eventual collapse of the front was due to the slowing down of inertial movement in combination with the passive sinking of fine particulates and evaporative cooling resulting in downward convection.

© 2007 Elsevier Ltd. All rights reserved.

**Keywords:** front; embayment; advection; False Bay; South Africa

## 1. Introduction

False Bay, to the east of Cape Town, South Africa (Fig. 1a) is a north–south orientated rectilinear embayment that is open to the south. Its size is approximately 35 × 30 km and its northern shore is characterized by a large dune field known colloquially as the Cape Flats. The water depth increases to approx 80 m at the bay mouth. Its east and west boundaries are formed by two prominent mountain chains; the Kogelberg

and Cape Peninsula respectively. The formation of a strong colour front along the False Bay northern shore occurs episodically and is well known to Capetonians and visitors alike. They are easily observable and have a sharp boundary between near-shore milky white-green water (MW-GW) and darker green-blue water (G-BW) offshore, which is more typical of ocean water. Personal observations have shown that although these fronts originate in the wide surf zone in the north-west of the Bay, very few are sufficiently well developed to sustain an expansion that extends as far south as Simon's Town. These colour fronts have been the subject of a previous study (Shannon et al., 1991). This comprehensive

\* Corresponding author.

E-mail address: howard.waldron@uct.ac.za (H.N. Waldron).

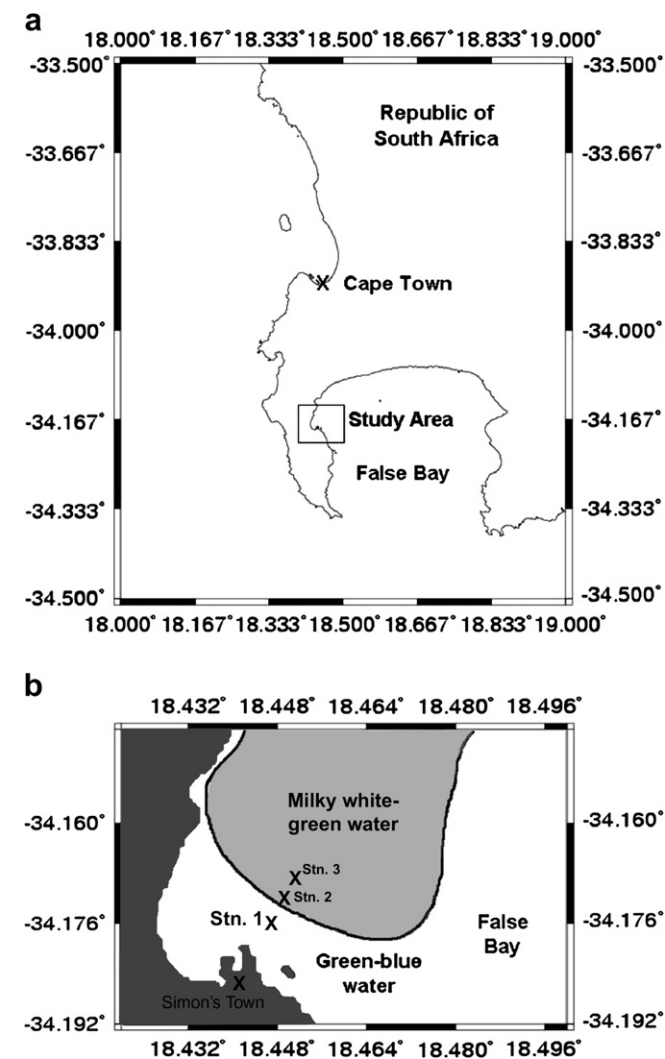


Fig. 1. (a) Study area. (b) Schematic representation of the front and positions of sampling stations.

paper concluded that land-based pollution from a local waste water treatment works was not a factor, nor was the erosion of fine materials from Swartklip (a rocky promontory on False Bay's north shore). In addition, the fronts were found to be not thermally driven, they were not simply surface features and, finally, the surf diatom, *Anaulus* was not a factor in their formation. Shannon et al. (1991) found that the waters either side of the fronts were identical in terms of their algal and faunal assemblages but that plants, animals and particles were more abundant in the MW-GW. Light-scattering resulted in the characteristic colouration. They noted the presence of calcium carbonate as an additional causative factor and stated that it could not be ruled out that the milky white colouration was due to the presence of aragonite needles. It was thought, however, that flocculation and rapid sinking would argue against this, given the post-formation persistence of the front. An opportunity arose in the early summer of 2005 to re-visit some of the findings of this previous study and draw conclusions relating to the formation dynamics, trajectory, content and persistence of this type of frontal feature.

## 2. Observation and methods

### 2.1. Observation

A prominent colour front was observed (from the shoreline) on the western side of False Bay close to Simon's Town (Fig. 1b) on the morning of 8 November 2005. It had the characteristic MW-GW to the north and much darker G-BW to the south (Fig. 2). The MW-GW was seen to be advancing steadily southwards but an accurate measure of its speed of advance was not possible. The surface transition from one water type to the other was immediate and the presence of floating matter (e.g. kelp fronds) at the frontal boundary indicated that it was strongly convergent. It was seen later that the front was also visible from satellite imagery. Fig. 3 shows a MODIS Terra quasi-true colour image (250 m resolution) from 8 November 2005 taken at the same time as this study. The MW-GW can be seen hugging the northern boundary of False Bay with a sharp east–west orientated front on the western side of the bay. It was necessary to react quickly and collaboration between the Institute for Maritime Technology (IMT) and the Department of Oceanography at the University of Cape Town resulted in the opportunistic cross-frontal sampling of this feature in the late morning of the same day. Three stations were conducted across the front using IMT's workboat (Sealab 1), one in the darker green-blue water (station 1, a few hundred meters from the leading edge of the front), the second (station 2) at a position judged to be the front interface and a third (station 3), a few hundred meters into the milky-white green side of the front (Fig. 1a). Positions were recorded using a Geographic Positioning System (GPS). Details are provided in Table 1. Sampling took place approximately 1 h after high tide and 36 h prior to a neap tide.

### 2.2. Methods

At each station a Sea-Bird Electronics portable CTD was deployed providing profiles of temperature, salinity, turbidity



Fig. 2. Photograph of the front taken from the western shore of False Bay 2 h prior to sampling.

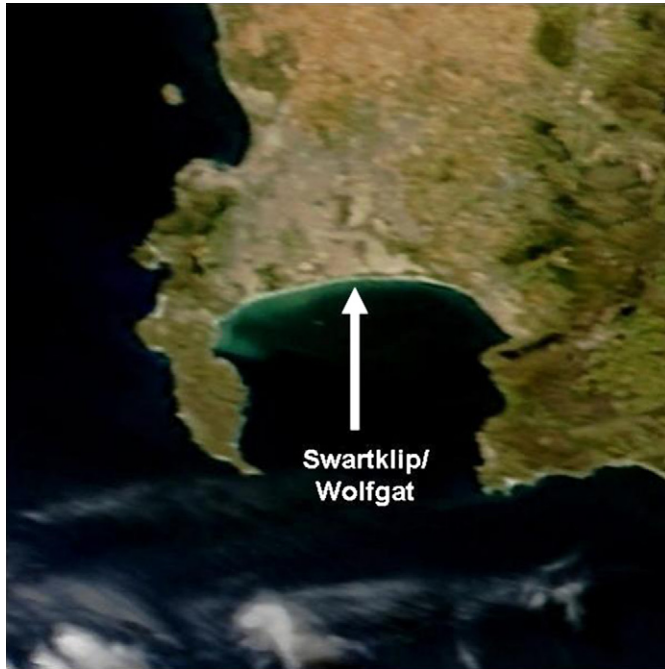


Fig. 3. MODIS Terra quasi-true colour image of False Bay, resolution 250 m. Image taken 8 November 2005, 10:00–11:30 h.

(optical backscatter) and dissolved oxygen. In addition, near-surface water samples were obtained for the later determination of nitrate-nitrogen, silicate-silica, chlorophyll *a* and suspended solids and examination of particulate material using a scanning electron microscope (SEM) and elemental dispersive x-ray (EDX) analysis. Nitrate and silicate concentrations were determined according to Grasshoff et al. (1983). Chlorophyll *a* was determined spectrophotometrically according to the method described in Parsons et al. (1984) and suspended solids were determined by filtration of samples onto pre-weighed, Whatman GFFs and subsequent drying and re-weighing. Water samples from the two water types were also filtered onto 1  $\mu\text{m}$  Nuclepore filters and used for examination with the SEM and EDX. This was done to provide a visual perspective of the particulate content of the two water types and to determine their respective elemental composition. Note that nutrients, suspended solids, chlorophyll *a* and SEM analysis were only conducted on one of the milky white-green samples (station 3) and the single green-blue station (1). With respect to suspended solids, duplicate analyses were performed on each of the milky white-green samples and four replicates were analysed on the G-BW. Meteorological data for the period preceding and during the frontal event were available from an automatic scientific recording weather station at the site of Roman Rock Lighthouse in Simon's Bay, owned and maintained by IMT. Sensors were located about 14 m above

sea level, approximately 1.5 km offshore. This site is important, especially in the context of this study, since it represents offshore weather conditions that often differ from those on land. It is also ideally placed, given its proximity to the colour front. Weather averages (10 min) were recorded in a memory module and relayed via HF radio transmission to the IMT offices nearby.

### 3. Results

#### 3.1. Meteorology

It is considered probable that weather conditions in the days leading up the event played a focal role in the establishment of the front. The period from 4–8th November (Julian days 308–312) was marked by persistent yet steadily increasing (5–15 m/s) southerlies. These conditions were coincident with raised and persistent air pressures (approx. 1020 hPa). These data are shown in Fig. 4. It is relevant to include the same variables for the preceding 2 weeks to establish the variable wind conditions in the period prior to the study.

#### 3.2. CTD data (temperature, salinity, turbidity and dissolved oxygen)

Profiles at each station have been plotted for temperature, salinity, turbidity and dissolved oxygen (percent saturation) and are shown in Fig. 5a–d. With the exception of dissolved oxygen saturation it is evident that station 1 (G-BW) was different in terms of its hydrographic structure compared to stations 2 and 3 (frontal and MW-GW). With respect to dissolved oxygen, the water column in both water types was supersaturated in the upper 2.5 m. A sharp oxycline was present at stations 1 and 2 between 2.5 m and 4.5 m below which the

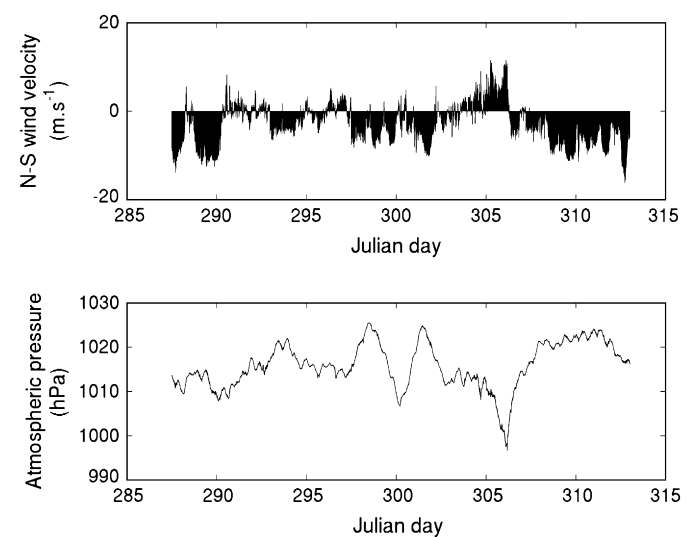


Fig. 4. Meteorological data in the period prior to frontal formation. Top diagram is a time series of the N-S velocity component of wind. Bottom diagram is a time series of atmospheric pressure. Note that Julian Day 290 was 17 October 2005. The front was observed and sampled on 8 November 2005 (Julian Day 312).

#### Q2 Table 1

Station ID	Latitude	Longitude	Local time (h)
1	34 10.9366 S	18 26.7011 E	10:03
2	34 10.7688 S	18 26.7819 E	10:07
3	34 10.6527 S	18 26.8607 E	10:25

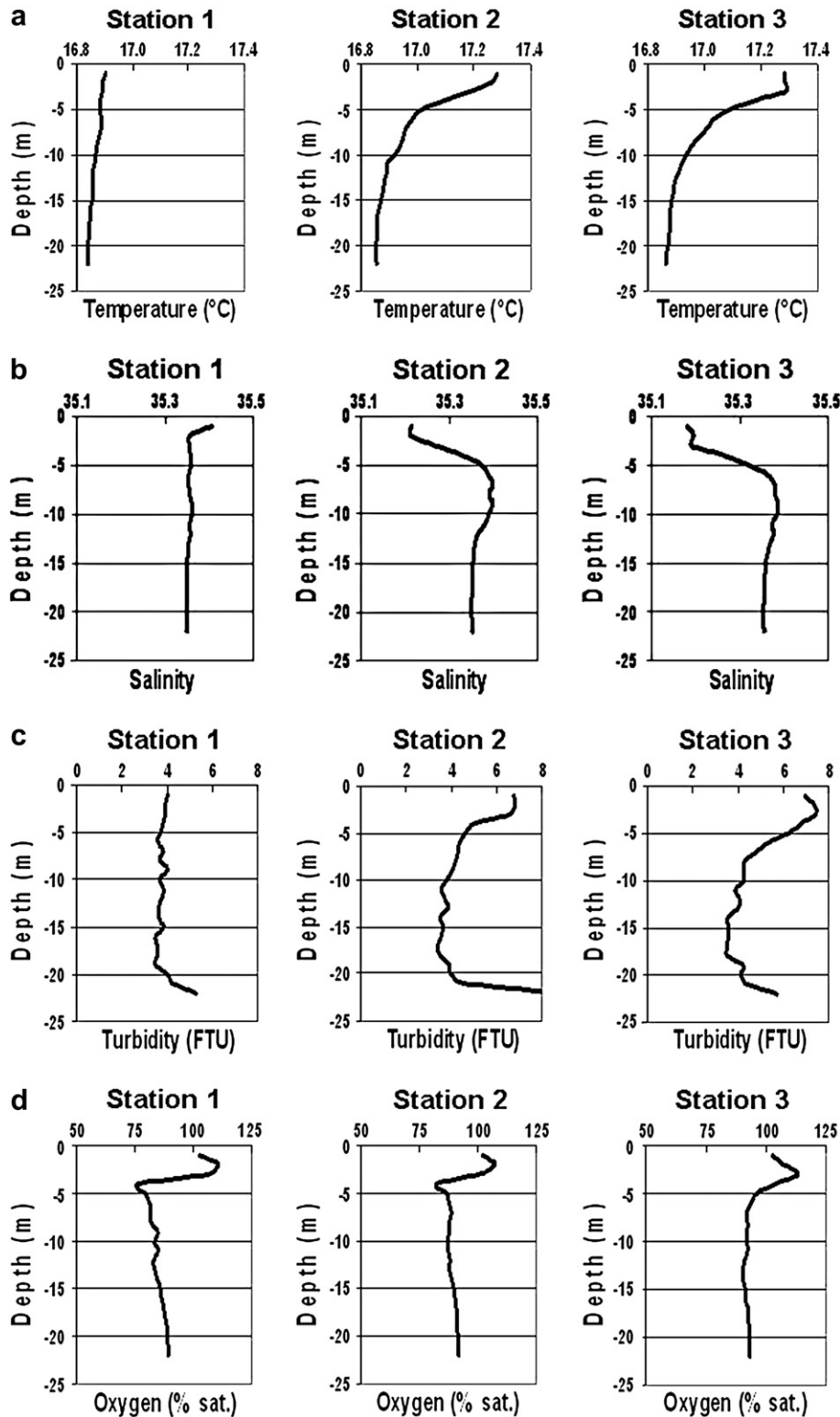


Fig. 5. Station 1 was in G-BW, station 2 was at the approximate interface, station 3 was in MW-GW. (a) Temperature profiles at stations sampled across the front. (b) Salinity profiles at stations sampled across the front. (c) Turbidity profiles at stations sampled across the front. (d) Dissolved oxygen saturation profiles at stations sampled across the front.

oxygen rose slightly to approx 82% at station 1 and 88% at station 2 forming a homogenous layer. The oxycline was less strong at station 3 and the bottom layer had an oxygen saturation of 92%. In respect of temperature, salinity and

turbidity (Fig. 5a–c), The G-BW at station 1 was isothermal (16.89–16.84 °C) isohaline (35.4 below 2 m) and isoturbid (3.5–4.0 FTU) except at the base of the water column, where turbidity increased. Station 2 (close to the frontal interface)

had a warm surface layer (17.3 °C max) below which temperature decreased with depth, achieving station 1 temperature at a depth of 12 m. This surface layer structure was mirrored in the salinity profile and was formed of water with lower salinity measurements than at station 1. The water column at station 2 had a turbid upper layer (6.8 FTU max.), which decreased to station 1 conditions below about 11 m. The structure at station 3 (within the MW-GW) was very similar to station 2 but the upper 3 m of the surface layer was well mixed. The maximum turbidity in the surface layer at station 3 was higher than at station 2 (7.4 FTU). These results show that at station 1, G-BW extended throughout the water column and at stations 2 and 3, the MW-GW (which overlaid the G-BW) was a warmer, (seemingly) fresher and more turbid layer extending down to a depth of 11–12 m. It is worth noting that the transect was plotted as a section for each of the variables but some subtleties in water column structure were lost due to interpolation by the software.

### 3.3. Plant nutrients (nitrate-N and silicate-Si) and chlorophyll *a*

The nitrate-N concentration in the MW-GW (station 3) was higher (8.0  $\mu\text{mol l}^{-1}$ ) than in the G-BW at station 1 (6.2  $\mu\text{mol l}^{-1}$ ) (Table 2). The pattern was the same with respect to silicate-Si (11.9  $\mu\text{mol l}^{-1}$  and 5.8  $\mu\text{mol l}^{-1}$  respectively). Chlorophyll *a* was also greater at station 3 (3.3  $\text{mg m}^{-3}$ ) than at station 1 (1.6  $\text{mg m}^{-3}$ ). These results are summarized in Table 2.

### 3.4. Suspended solids

There was no discernible difference in the suspended solids content ( $\text{mg l}^{-1}$ ) between the two waters.

The stations in the MW-GW (station 3) had suspended solid concentrations of 16.3, 14.2, 14.7 and 15.1  $\text{mg l}^{-1}$ ; mean value 15.1  $\text{mg l}^{-1}$ .

The stations in the G-BW (station 1) had suspended solid concentrations of 14.4, 16.0, 13.7 and 16.7  $\text{mg l}^{-1}$ ; mean value 15.2  $\text{mg l}^{-1}$ .

This was a surprising result given the visual impression of respective sediment loads and the turbidity differences between the two water types. An explanation of this apparent inconsistency is given later.

### 3.5. SEM images

Two images from the MW-GW and two from the G-BW are shown in Figs. 6 and 7 respectively. In each case, the upper image was 1000 $\times$  and the lower was 7000 $\times$ . The MW-GW

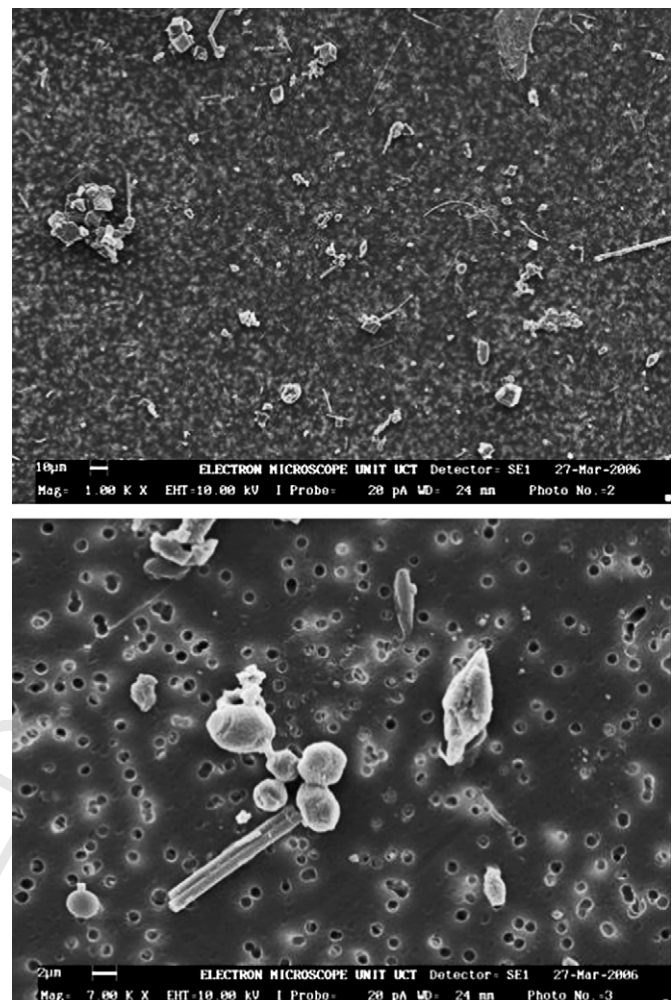


Fig. 6. Scanning electron microscope images of MW-GW particulates at  $\times 1000$  (upper image) and  $\times 7000$  (lower image) magnification.

(Fig. 6) contained fragmentary material with particle size of 2–10  $\mu\text{m}$ . The G-BW (Fig. 7) had fewer particles but of a similar size range. It was noted (Fig. 7) that the material in this sample was less fragmentary. It has not been possible to give a definitive identification of the particulates in either water type, however the particles in the G-BW (Fig. 7) appear to have a greater coherency than those in the MW-GW (Fig. 6).

### 3.6. EDX analysis

EDX analysis for a comprehensive suite of elements was undertaken on the particulate fraction of both water types. The EDX analysis was able to detect a percentage by weight composition for oxygen, sodium, magnesium, aluminium, silicon, sulphur, chlorine, potassium, calcium, titanium, iron and zinc. The relevant elements for the purpose of this study were considered to be silicon and calcium. The former would be representative of the presence of diatoms (and possibly sand) and the latter, an indication of the presence of calcium carbonate derived material. The mean percentage-by-weight results for these elements are given in Table 3.

Table 2

	Station 1	Station 3
Nitrate-N ( $\mu\text{mol l}^{-1}$ )	6.2	8.0
Silicate-Si ( $\mu\text{mol l}^{-1}$ )	5.8	11.9
Chlorophyll <i>a</i> ( $\text{mg m}^{-3}$ )	1.6	3.3

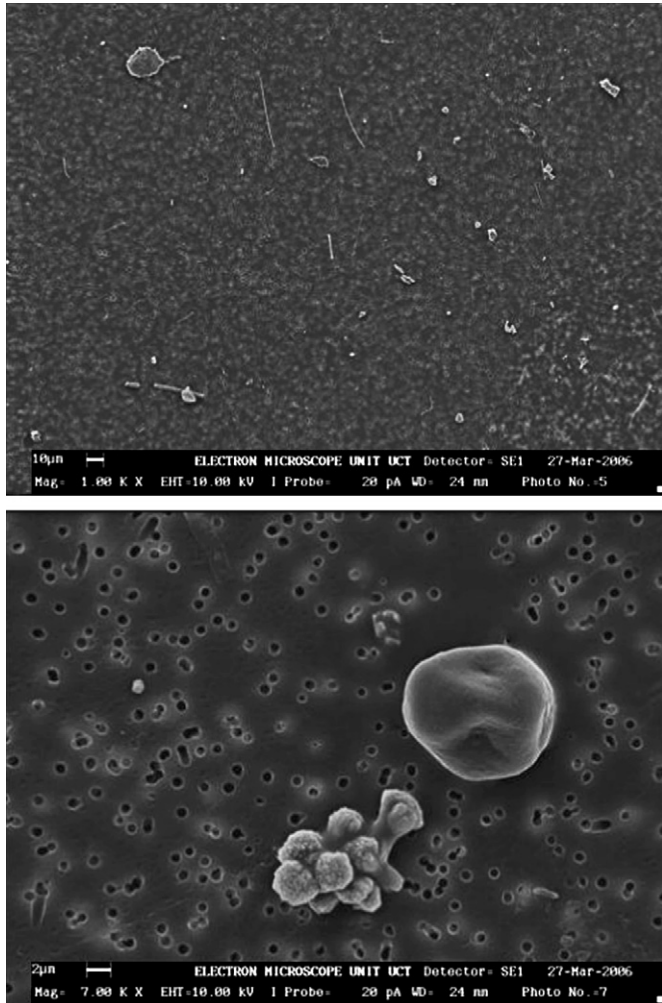


Fig. 7. Scanning electron microscope images of G-BW particulates at:  $\times 1000$  (upper image) and  $\times 7000$  (lower image) magnification.

It can be seen that the particulate content of the G-BW was silicon-enriched and the particulates of the MW-GW were calcium-enriched. The enrichment was much greater in respect of calcium in the MW-GW.

#### 4. Discussion

The front observed on the western side of False Bay on 8 November 2005 was very evident from a visual perspective (Figs. 2 and 3). Having sampled across the feature it was also evident in terms of certain hydrographic variables, *inter alia* temperature, salinity and turbidity (Fig. 5a–c). The front was not as evident in respect of dissolved oxygen measurements (Fig. 5d). The dissolved oxygen structure across the front indicated supersaturation in the upper water column; this was enhanced at station 3, which was at a position further

Table 3

	Milky white-green	Green-blue
Silicon	17.8	27.9
Calcium	24.8	6.6

within the MW-GW. This oxygen signature is in accord with the observed readings of chlorophyll *a* ( $3.3 \text{ mg l}^{-1}$  in the MW-GW and  $1.6 \text{ mg l}^{-1}$  in the G-BW). Plant nutrients (nitrate and silicate) were non-limiting on both sides of the front although the lower concentration of silicate in the G-BW may imply a higher diatom biomass.

In respect of the physical structure across the front (temperature, salinity and turbidity), it was felt appropriate to make turbidity the starting point. The visibility of the advancing front was based on the sharp difference in colour between the two water bodies. The MW-GW was assumed to carry a sediment load in suspension that differed markedly from the G-BW. Before attempting to interpret the coincident temperature and salinity structure across the turbidity front, the difference in cross-frontal particulates should be addressed. The samples that were filtered onto GFFs for suspended solid analyses gave the visual impression of more filtered material in the case of MW-GW than G-BW. The SEM images (Figs. 6 and 7) confirmed this impression. In both types of water, the size range was 2–10  $\mu\text{m}$ , however the MW-GW particulates were more fragmentary (Fig. 6) compared to the G-BW (Fig. 7). The results from the EDX analysis indicated that the MW-GW was relatively enriched (nearly fourfold) in calcium whereas the G-BW was silicon-enriched (although to a much lesser extent). It is the authors' contention that the MW-GW particulates were rich in calcium carbonate in some form, e.g. aragonite, calcite or limestone and that the G-BW contained more siliceous material, probably of diatom origin. This may help to explain the surprising results obtained with respect to suspended solids content. There was no discernible difference in the weight of suspended solids per unit volume between the two water bodies on either side of the front. This was paradoxical given the visual evidence of more particulates per volume of water in the MW-GW (*in situ* appearance, turbidity values, SEM photographs and discolouration of the GFF filters). If it is accepted that the MW-GW had a greater sediment load than the G-BW and further, that the weight per litre of particulate material in both water types was indistinguishable, then the only logical explanation is that the particulate material in the MW-GW was less dense than its G-BW counterpart. Certain forms of biogenic calcium compounds have a density that would be consistent with this explanation. For example, the dry density of biogenic calcium carbonate is quoted as  $1.00 \text{ g cm}^{-3}$  (Janik and Hood, 2000) and fine chalk (e.g. limestone) has a density of  $1.1 \text{ g cm}^{-3}$  ([http://www.simetric.co.uk/si\\_materials.htm](http://www.simetric.co.uk/si_materials.htm)). Silica, on the other hand (occurring in greater abundance in the G-BW) has a density of  $2.6 \text{ g cm}^{-3}$ . These factors may help to explain why the sediment load in the MW-GW does not readily sink out of the surface layer and hence persists as a colour front. It is argued above that this water's particulate content consists (to a large extent) of calcium-derived material that may have a density of around  $1.00 \text{ g cm}^{-3}$ . This would be slightly buoyant in ambient seawater (density  $1.026 \text{ g cm}^{-3}$ ) and through turbulence and advection, would form part of the hydrodynamic movement of the frontal waters. It is the intention of future studies to test this contention by adopting a sampling

strategy that will permit the direct determination of the density of particulate material in the MW-GW and G-BW respectively. It should be noted that the weight of suspended solid per volume in the MW-GW (mean  $15.1 \text{ mg l}^{-1}$ ) was similar to that found by Shannon et al. (1991) although their non-frontal water suspended solid content was less than the present study.

It was noted that the temperature and salinity profiles obtained across the front (Fig. 5a and b) showed the same physical structure as the profiles of turbidity (Fig. 5c). The question arose as to whether the source of the MW-GW was warmer ( $+0.4^\circ\text{C}$ ) and fresher ( $-0.2$  PSU) or have these effects occurred post-formation. The satellite image of the MW-GW in False Bay (Fig. 3) shows that it occurred as a band, hugging the coast and sweeping south on the western side of the bay. It has been established that the mean suspended solid content of the MW-GW was  $15.1 \text{ mg l}^{-1}$ , composed of particles in the  $2\text{--}10 \mu\text{m}$  range and more abundant than its B-GW counterpart. It is suggested that there are two mechanisms, possibly acting in concert, that made this water warmer. It is well established from web-based water quality documentation (<http://www.scc.rutgers/coastweb>; <http://www.duluthstreams.org>) that high suspended particle concentrations can cause an increase in surface water temperature due to the absorption of heat from sunlight. In the present case this effect may be reduced by the reflection of light due to the whitish colouration of the water. It is also possible that the waters along the north edge of False Bay, within and close to the shallow surf zone (the source of the MW-GW), would be heated to a greater extent than waters further offshore. The neutrally or negatively buoyant particulate material contained in a relatively warm water body would inevitably move over the more dense G-BW as it begins its southward movement from the north-west corner of False Bay. This pattern of events may also help to explain the eventual collapse of the front. There is no obvious reason, however, why the MW-GW water should be less saline than the G-BW water. One possible explanation is that the water recently originated from a small upwelling cell that occurs in the south eastern corner of False Bay during strong south east winds, however, NOAA AVHRR images of False Bay in the 3 days preceding this study show no such occurrence. In fact, the upwelling cell was developing on the day that the colour front was sampled and would have had no influence. An alternative explanation for the MW-GW having a lower salinity is that it was an artefact of the CTD's conductivity measurement. The conductivity cell measures conductivity over a specific length scale. Sediment present in the water would effectively reduce the length scale and hence reduce the conductivity reading. The water had a fine sediment load which "might easily be expected to drive the measured salinity fresh of correct. The  $0.2$  [psu] effect in surface salinity seems plausible if [calcium carbonate] concentrations are high." (Dr Norge Larson, Sea-Bird Electronics, Inc., personal communication). It is contended that the latter explanation is correct and that, when sampled, there was no discernible salinity difference between the two water types. If the MW-GW was warmer than, but of the same salinity as G-BW, this may provide a mechanism for the eventual collapse of the

front. As the front continued to advect southwards, the expected evaporative cooling of a turbid water body would, ultimately, create a high salinity environment in the surface. This would be more dense and hence sink (Wolanski, 1986).

Having discussed the results of the current study, it is now timely to re-visit the Shannon et al. (1991) paper and make certain comparisons with their findings. The current work is in agreement in several respects:

- Land-based pollution from a local waste water treatment works is not a factor in the formation of the colour front.
- Surf diatoms (Anaulus) play no part in frontal formation.
- The characteristic colouration of the MW-GW is a result of light-scattering and the colouration could be due to the presence of a calcium based compound.

There are, however, some points of departure:

- The current study found that the MW-GW was about  $0.4^\circ\text{C}$  warmer than its adjacent water and was a relatively shallow feature overlying the G-BW. It had previously been suggested that the front was not thermally driven and was not simply a surface feature.
- The previous study stated that waters either side of the front were identical in algal and faunal assemblage but plants, animals and particles were more abundant in the MW-GW. The electron microscope images (Figs. 6 and 7) show the two waters to have differing abundances and types of particulate content and, further, the MW-GW was rich in calcium whereas the G-BW was relatively rich in silica.
- Shannon et al. (1991) ruled out aragonite needles as forming the MW-GW on the basis of frontal persistence versus flocculation and rapid sinking. This study is in agreement, however it is contended that an alternative form of calcium carbonate was responsible for MW-GW water formation. It was found that the particulate content of the MW-GW was greater than in the G-BW, but each water type had a similar mass of suspended solid content. Since density is the ratio between mass and volume, this means that the particulate material in the MW-GW was less dense than the particulate content of the G-BW. The MW-GW was rich in calcium and whilst there was no SEM evidence of aragonite needles it is possible that the calcium compound in the MW-GW was sufficiently low in density to maintain positive buoyancy.

It may be possible to make some inferences regarding the pre-conditions required for frontal formation and the source of frontal material. Fig. 4 shows a 4-day period of sustained winds from the south with high atmospheric pressure. The first 3 days of this period occurred at the end of a spring tide cycle. In these circumstances the strong onshore wind would result in a wide surf-zone (order of  $>1$  km) and the sea would advance higher up the shoreline than the predicted tide. An example of the surf zone conditions under these winds is shown in Fig. 8.



Fig. 8. Typical surf zone conditions along the north shore of False Bay under southerly wind conditions.

**Wolfgat cliffs**



**Pipe nodules of calcrete  
Wolfgat**



**Wolfgat – crumbling cliffs**



**Cliffline exposures of Estuarine  
sands Swartklip**



Fig. 9. Four photographs of the sea–land interface at Wolfgat and Swartklip (courtesy of University of Cape Town, Geology Department).

Du Plessis and Glass (1991) provide a comprehensive study of the geology of False Bay. On the basis of (*inter alia*) side-scan sonar and sediment sampling they were able to identify physiographic terrains and sedimentary assemblages. Side scan sonar results showed that along the western half of the northern edge of False Bay (their physiographic terrain 9) at depths of less than 30 m, the sea bed comprised of calcrete or calcrete with a thin sediment cover. Grab samples in the same zone (their sedimentary assemblage Q2) were identified as consisting of white, friable limestone. This sector of False Bay coincides with the spatial coverage of the frontal waters shown in Fig. 3. Note that the calcrete horizon has a prominent terrestrial outcrop at Wolfgat and Swartklip (location shown in Fig. 3). Other geological studies of relevance have been undertaken along the northern edge of False Bay. Singer and Fuller (1962) found that “at Swartklip the beach narrows at the base of the cliffs and is absent beneath the headland.” The cliff material was identified as unconsolidated shelly sand and



913 a thin crust of well-cemented calcareous tufa that had formed  
914 as a result of calcium carbonate precipitation from groundwa-  
915 ter during (in geological time) an arid period. They further  
916 state that wave and wind action undercut this boundary and  
917 “the beach is strewn with great blocks of calcareous sand-  
918 stone.” Barwis and Tankard (1983) support these findings in  
919 their observation that beach rock (flatbedded sandstone capped  
920 by calcrete) was present intermittently in the intertidal. Four  
921 photographs have been included from this area (Fig. 9  
922 courtesy of University of Cape Town, Geology Dept. [http://](http://web.uct.ac.za/depts/geolsci/dlr/106s_03/index.html)  
923 [web.uct.ac.za/depts/geolsci/dlr/106s\\_03/index.html](http://web.uct.ac.za/depts/geolsci/dlr/106s_03/index.html)).

924 In summary, it is proposed that frontal formation relies on  
925 local geology. This is one of a suite of possible causative fac-  
926 tors that may be worth considering in other coastal colour  
927 front studies. In the present case, there is abundant calcareous  
928 source material in shallow waters and at the land/sea interface  
929 on the northern boundary of False Bay to form the MW-GW  
930 observed as a colour front in November 2005. The wide surf  
931 zone occurring during strong southerly wind conditions has  
932 the potential to erode the inter- and sub-tidal deposits of cal-  
933 crete, an effect possibly enhanced by erosion of beach-strewn  
934 calcareous sandstone at Swartklip during Spring Tide. This  
935 MW-GW would be warmer due to its presence in the shallow  
936 near-shore, making it less dense than waters further offshore  
937 (the GB-W); further warming may result *per se* from its fine  
938 particulate content. The advection of this water, initially  
939 wind-driven and subsequently, under its own inertia, would  
940 then be constrained by the northern and western boundaries  
941 of False Bay resulting in the MW-GW flowing over the  
942 GB-W in an anti-clockwise trajectory seen in Fig. 3. Reasons  
943 for the eventual collapse of the front are conjectural but may  
944 be due to the gradual slowing down of inertial movement in  
945 combination with the passive sinking of fine particulates and  
946 evaporative cooling, which would result in downward convec-  
947 tion. It is interesting to note that offshore sediment samples in  
948 the north-west corner of False Bay and to the south of Simon’s  
949 Town (Du Plessis and Glass, 1991) consisted of white friable

957 limestone. Under different strengths of forcing, these locations  
958 are consistent with the probable zones of frontal collapse. The  
959 mechanism by which the front collapses provides one of sev-  
960 eral suitable research foci for planned future research.  
961

### Acknowledgements

962 The authors would like to thank staff from the Institute for  
963 Maritime Technology for infrastructural support and members  
964 of the UCT Departments of Oceanography and Geological  
965 Sciences for useful discussions during the preparation of this  
966 paper. Names include Ms Sanette Gildenhuys, Ms Benita Mar-  
967 itz, Prof. Frank Shillington, Prof. Vere Shannon, Dr John  
968 Rogers and Mr Neil Swart. Thanks also to Prof. Dave Reid,  
969 UCT Department of Geological Sciences, for permission to  
970 use his photographs of Swartklip and Wolfgat.  
971

### References

- 972 Barwis, J.H., Tankard, A.J., 1983. Pleistocene shoreline deposition and sea  
973 level history at Swartklip, South Africa. *Journal of Sedimentary Petrology*  
974 53 (4), 1281–1294.  
975 Du Plessis, A., Glass, J.G., 1991. The geology of False Bay. *Transactions of*  
976 *the Royal Society of South Africa* 47, 495–517.  
977 Grasshoff, K., Ehrhardt, M., Kremling, K., 1983. *Methods of Seawater*  
978 *Analysis*, second ed. Verlag Chemie, Weinheim, Germany, 419 pp.  
979 Janik, A.G., Hood, J.A., 2000. Data report: index properties, calcium carbon-  
980 ate, and opal content of core 167-1016B-17H<sup>1</sup>. In: Lyle, M., Koizumi, I.,  
981 Richter, C., Moore Jr., T.C. (Eds.), *Proceedings of the Ocean Drilling*  
982 *Program, Scientific Results*, 167.  
983 Parsons, T.R., Maita, Y., Lalli, C.M., 1984. *A Manual of Chemical and*  
984 *Biological Methods for Seawater Analysis*. Pergamon Press, 173 pp.  
985 Shannon, L.V., Hennig, H.F.-K.O., Shillington, F.A., Bartels, A., Swart, D.H.,  
986 1991. Colour fronts in False Bay: origin, development and implications.  
987 *Transactions of the Royal Society of South Africa* 47, 447–469.  
988 Singer, R., Fuller, A.O., 1962. The geology and description of a fossiliferous  
989 deposit near Swartklip, False Bay. *Transactions of the Royal Society of*  
990 *South Africa* 36, 205–211.  
991 Wolanski, E., 1986. An evaporation-driven salinity maximum zone in Austra-  
992 lian tropical estuaries. *Estuarine, Coastal and Shelf Science* 22, 415–424.  
993  
994  
995  
996  
997  
998  
999  
1000